# SPATIAL RESOLUTION AND ACCURACY OF INTERFEROMETERY OF MICROSCOPIC PHASE OBJECTS

V. F. Klimkin and G. S. Lomakin

UDC 541.126

At the present time, optical recording methods have been substantially developed in connection with investigations of physical processes in gases, liquids, and high-temperature plasma with limiting temporal and spatial resolution [1]. One of the main elements of the optical setup is the optical system which forms the image of the object under study on a screen. Because of diffraction, aberrations, and focusing inaccuracy the edges of each detail of the object are smeared, which limits the resolution and accuracy of the measurements. The spatial resolution has therefore been analyzed in a number of works (for example, [2, 3]). As a rule, however, the imperfection of the images asssociated with the diffraction of light was studied, though in most practical cases the spatial resolution is determined by the errors (aberrations) introduced by the optical elements. Abbe's diffraction theory of the formation of optical images [4] was developed for flat periodic structures. while real objects are more complicated and three-dimensional. The light incident on such an object is reflected, scattered, and transmitted, which can change and complicate the diffraction pattern of the intensity distribution on the screen. The question of the resolution of details in an extended phase object is especially important; this is associated with the development of optical methods (schlieren methods, interferometery) for studying microscopic objects.

Thus in [5] microscopic perturbations with characteristic size of $\sim 10^{-2}$ cm were studied with the help of optical interferometry, which enabled obtaining quantitative results concerning the initial stage of the development of an electrical discharge in liquid dielectrics. A theoretical analysis of the possibilities of interferometry in studying nonstationary physical processes is performed in [6].

In this paper we present the results of an experimental analysis of the spatial resolution and accuracy of interference measurements in photographic recording of extended phase microscopic objects.

1. Experimental Setup and Measurement Procedure. The layout of the setup used to perform the optical measurements with the help of a Mach–Zender interferometer is given in [5]. An LG-38 helium–neon laser was used as the illumination source. The experiments were performed on cylindrical microscopic objects with a diameter of 50-400 μm, which were obtained by heating samples of fused quartz in the flame of a burner and subsequently drawing them out. The dimensions of the objects were determined with a microscope to within ~1-2 μm. In order to decrease the large change in the index of refraction at the quartz–air boundary, the objects were placed in a special chamber filled with carbon tetrachloride, whose index of refraction at a temperature of ~293°K is somewhat higher than the index of refraction of fused quartz. Since the index of refraction of $CCl_4$ increases by ~100 times more than for fused quartz when the temperature is increased by 1°K, by changing the temperature of the liquid it was possible to regulate smoothly the magnitude of the jump in the index of refraction. The temperature dependence of the index of refraction of carbon tetrachloride was determined with the help of an IRF-23 Pul'frich refractometer for a wavelength of $\lambda_0 = 0.633$ μm (with a measurement error of $\sim 10^{-4}$). The error in the measurements of the temperature was equal to ~0.1°K. The index of refraction of the microscopic objects was determined with the help of an interferometer, adjusted to fringes of finite width. The liquid was heated smoothly up to the temperature at which the interference fringes passing through the object are not distorted. In this case, the average value of the index of refraction of the sample is equal to the index of refraction of the liquid at the given temperature. The accuracy of this method is determined by the accuracy of the measurement of the displacement of the interference fringes. For an error in the measurement of the displacement of the fringes equal to $\Delta k \leq 0.1$ fringes and a geometric path length of the ray in the nonuniformity equal to $L \sim 400$ μm, the error in the measurement of the index of refraction is equal to $\Delta k \lambda_0 / L \leq 2 \cdot 10^{-4}$, which is comparable to

Novosibirsk. Translated from Zhurnal Prikladnoi Mekhaniki i Tekhnicheskoi Fiziki, No. 2, pp. 40-45, March-April, 1985. Original article submitted January 25, 1984.

0021-8944/85/2602-0187$09.50  

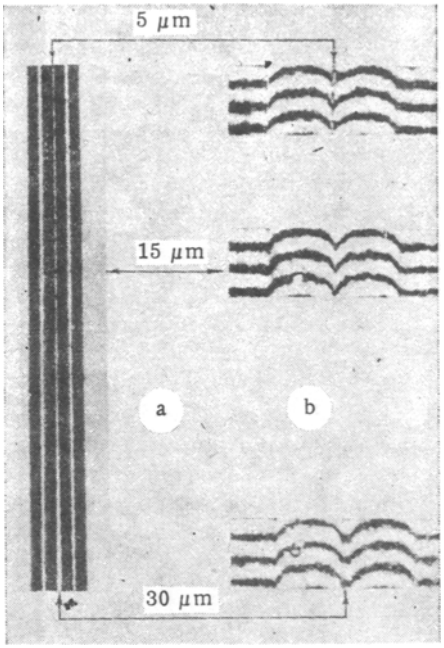


Fig. 1

the error of a refractometer. It should be noted that the selected microscopic objects model the physical processes with a jump-like change in the density at the boundary and are characterized by sharp (near the boundary) and smooth (near the axis) changes in the phase of the light wave. The objects were focused on high-resolution film (Mikrat-300, FPGV-2) with the help of the Yupiter-11 photographic objective (the relative aperture is 1:4 and the focal length is 135 mm). The setup described above permits obtaining different patterns of displacements of interference fringes by changing the index of refraction of the liquid. The distribution of the index of refraction in the microscopic object under study was determined from the measured displacement of the interference fringes by solving Abel's integral equation by the method of statistical regularization [6].

2. Experimental Results and Discussion. To evaluate the spatial resolution of the interferometric setup (taking into account the properties of the transmitting optical system and the photographic material), a model object whose size varied in the transverse direction was prepared. For this, two quartz cylinders with a diameter of less than 200 μm were placed in the same plane at a small angle to one another, so that the distance between them increased smoothly from 5 to 30 μm. The photograph of the model object in air, obtained with the help of a microscope, is shown in Fig. 1a. Figure 1b shows the pattern of interference fringes, corresponding to different sections of the object in carbon tetrachloride. The qualitative difference in the behavior of the interference fringes is evident. With a transverse size of the object of ~5 μm, a break is observed in the interference fringes, which makes it impossible to determine the phase of the light wave. As the distance between the cylinders is increased, the fringe pattern changes and it becomes possible to follow the course of the interference fringes in this region. It follows from the results obtained that the characteristic size of an element in the plane of the object, phase information about which is perceived by the optical system of the interferometer, is equal to about 15 μm. We shall estimate the diffraction limit of the resolution. In this case, the distance between two objects which can just be resolved (with a circular opening on the objective) is determined by the expression [4]

$$d \simeq A\lambda_0 / (n \sin \theta),$$

where $\lambda_0$ is the wavelength of the light in a vacuum, n is the index of refraction of the medium, and $2\theta$ is the aperture of the objective. The numerical factor A in this expression is equal to 0.6 (according to Rayleigh's criterion) or 0.8 (according to Abbe's theory). For $\lambda_0 = 0.63$ μm, $n = 1.46$, $\sin\theta \sim 8 \cdot 10^{-2}$, corresponding to the conditions of the experiment, $d \sim$ 3-4 μm. This is four to five times less than the real resolution of the interferometer. It follows from the estimates that the spatial resolution is determined by the aberrations of the objective and becomes comparable to the diffraction limit of the resolution only for $\theta \sim 2 \cdot 10^{-2}$ rad. Further decrease of the angle $\theta$ leads to additional distortion of the image in accordance with the diffraction theory.

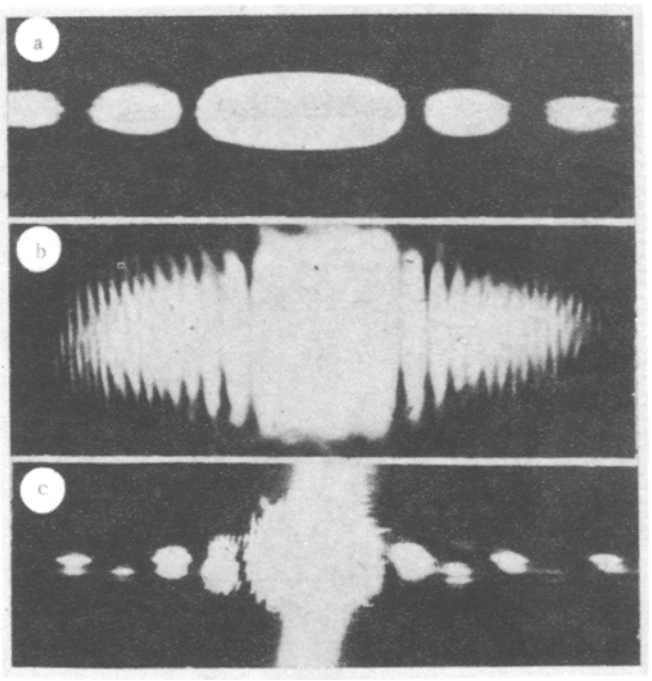


Fig. 2

As noted in [5], the optical layout used enabled obtaining a simultaneously focused shadow image of optical perturbations with large gradients of the index of refraction. For this reason, the experiments were also performed with objectives in air. They showed that using schlieren photographs it is possible to observe the existence of two objects separated by a distance of ~5 μm. In this case, the relative depth of the "trough" in the total illumination pattern from the results of photometric measurements constituted 30% and did not change significantly when the angle θ was decreased to $\sim 3 \cdot 10^{-2}$ rad. The results obtained indicate that the estimates of the diffraction limit of resolution must be treated with great care. This is linked to the arbitrariness of Rayleigh's criterion. A rigorous estimate of the limiting resolution in Abbe's theory is also complicated. As is well known, Abbe's theory examines diffraction of light by an object and the quality of the image is determined by the number of interfering beams corresponding to the diffraction maximum of different orders. When real three-dimensional objects are illuminated by coherent radiation, however, additional waves which can interfere with the "reference" plane and diffracted waves appear. Figure 2a shows a typical pattern of the distribution of the intensity with Fraunhofer diffraction by a flat slit 50 μm wide. For diffraction by a wire of the same size the general form of the pattern is preserved. As can be seen from Fig. 2b, however, the appearance of an additional interference structure is characteristic for the central maximum. The diffraction pattern produced by a quartz filament 80 μm in diameter is even more complicated (Fig. 2c). In addition to the modulation of the intensity of the central maximum, the character and the structure of the secondary maxima change. The results presented lead to the conclusion that a more accurate theoretical estimate of the diffraction limit of resolution must be made taking into account the description of the diffraction of light by three-dimensional structures.

In the interferometric study of phase microscopic objects, the question of the accuracy of the measurements of the phase shifts is also important. As an illustration, Fig. 3a shows a typical interferogram of a cylindrical sample consisting of fused quartz, obtained on a model setup and corresponding to an average change in the index of refraction equal to $\langle \Delta n \rangle = 9 \cdot 10^{-4}$. The diameter of the sample was measured with the help of a microscope and is equal to 405 μm. Twenty fringes, encompassing a zone of the object with an extent of about 2 mm, were selected in order to analyze the accuracy of the measurements of the relative phase shift (displacements of the interference fringes). Since the perturbation occupies a small part of the interference field, the reference interference fringes extended into the region occupied by the object. The symmetry axis y was drawn through the center of the object. Lines parallel to the symmetry axis were drawn on both sides of the symmetry axis with an interval of 1 mm (about 30 μm in the plane of the object). The displacements of the interference fringes were determined with the help of a magnifying glass with a division of 250 μm

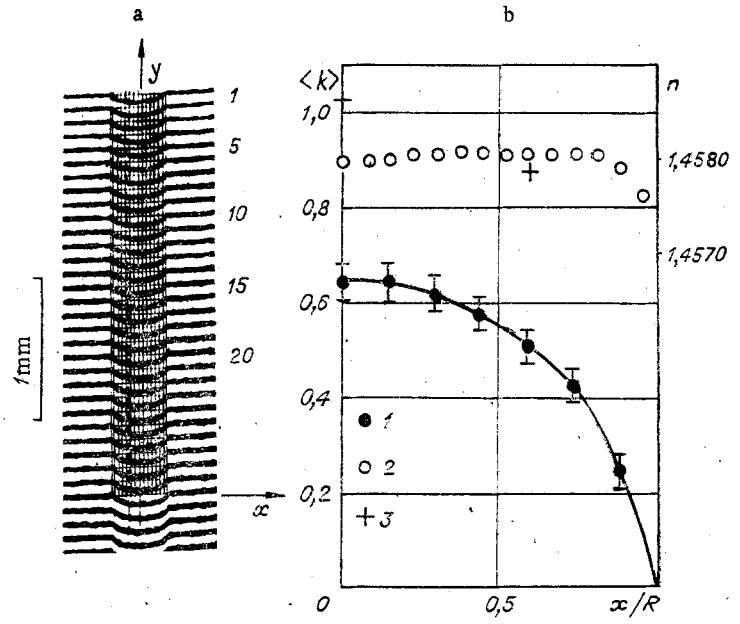


Fig. 3

at the points of intersection of these lines with the dark interference fringes. The measurements were performed on both sides of the axis, and the average values were determined. Thus, in processing 200 interference fringes, 40 measurements were performed for each "impact" parameter x. Figure 3b (the points 1) shows the relative displacements of the interference fringes <k>, averaged over 40 points, as a function of the dimensionless parameter x/R, where R is the radius of the cylinder. Under the assumption that the main error in the measurements is the random error and the errors obey the normal distribution law, we shall estimate the magnitude of the rms error of the separate measurement. Figure 3b (points 1) shows the magnitude of this error, corresponding to a confidence probability of 0.95. It is evident that for different values of x/R it is equal to ~0.03-0.06 fringes. For an error in the measurement of the displacement of the interference fringes equal to ~0.05 fringes, the relative error under the conditions of the given experiment is equal to $\lesssim 8\%$ for the center of the object and 25-30% near the boundary. It follows from a comparison of the average values <k> with the quantities corresponding to $\langle \Delta n \rangle = \text{const}$ that the change in the index of refraction is not the same within the object. This is apparently attributable to the fine structure appearing during the preparation of the microscopic samples. It is interesting to determine $\Delta n$ from the values of <k> obtained and, knowing the temperature of the liquid, transform to the distribution of the index of refraction of quartz. The results of the reconstruction of the profile of the index of refraction by the method of statistical regularization are shown in Fig. 3b (the points 2). It is evident that the profile indeed does not correspond to a stepped profile. However, the average of the reconstructed values of the index of refraction of quartz 1.4580 agrees well with the average obtained earlier 1.4579, which confirms the quite high reliability of the method. Figure 3b (the points 3) also shows the measurements of the index of refraction for a sample with a diameter of 52 μm. It should be noted that the results are in qualitative agreement, indicating that the geometric-optics approximation can be applied to such objects. A more accurate analysis undoubtedly requires the use of wave optics.

It should be noted in conclusion that the quantitative results obtained in this work are close to the limiting results. Under the conditions of a specific physical experiment, an additional analysis, associated with the motion of the object, its extent, focusing inaccuracy, etc., is required.

The authors thank A. B. Gulakov for assistance in performing the work.

## LITERATURE CITED

1. V. F. Klimkin, A. N. Papyrin, and R. I. Soloukhin, Optical Methods for Recording Fast Processes [in Russian], Nauka, Novosibirsk (1980).
2. U. Ascoli-Bartoli, "Plasma diagnostics based on refractivity," in: Plasma Physics, Int. Atomic Energy Agency, Vienna (1965).

3. G. V. Sklizkov, "Lasers in high-speed photography," in: Laser Handbook, North Holland, Amsterdam (1972).
4. M. Born and E. Wolf, Principles of Optics, Pergamon (1975).
5. V. F. Klimkin and A. G. Ponomarenko, "Study of impulsive electric breakdown of liquids with the help of optical interferometry," Zh. Tekh. Fiz., 49, 9 (1979).
6. V. F. Klimkin and V. V. Pikalov, "Possibilities of microinterferometry in the study of nonstationary processes," Zh. Prikl. Mekh. Tekh. Fiz., No. 3 (1979).

# USE OF THERMAL TRANSDUCERS FOR MEASURING THE MOLECULAR VELOCITY DISTRIBUTION FUNCTION

S. G. Mironov and A. I. Sedel'nikov

UDC 539.198

1. In recent years, thermal transducers (bolometers [1-6] or pyroelectrics [7, 8]) have been used as detectors in performing molecular beam measurements. The quantity to be recorded here is the flux of the thermal energy developing as a result of interaction between the beam molecules and the surface of the transducer's sensing element. Modern thermal transducers have a high sensitivity to small molecular fluxes (up to $10^{12}$ molecules/($m^2$·sec) [1]) along with rather low inertia (the thermal relaxation time amounts to less than $10^{-4}$ sec [1, 5]). These transducers are espeically useful for detecting molecules with excited internal degrees of freedom in the excitation energy range of up to 1 eV, where devices based on the effect of Auger electron emission are inoperative. There is the possibility of investigating the processes of intrinsic molecular energy excitation and relaxation [4-6, 8]. Inclusion of a thermal transducer in the flight-time measuring circuit [9, 10] provides information on the effect of intrinsic energy relaxation on the molecular kinetic energy without adding to the complexity of the experimental equipment. In the case of molecular photoexcitation by laser radiation [4, 8], it is possible to use a generator of short laser pulses instead of the mechanical modulator in the flight-time circuit. The use of a bolometer as the detector in a flight-time measuring circuit was described in [5]. An expression relating the molecular velocity distribution function to the time dependence of the temperature increment of the bolometer's sensing element was also given there. Several simplifying assumptions were used in this case. In the more general formulation given here, we have derived an integral equation relating the molecular velocity distribution to the electric signal received from the output of the thermal transducer (bolometer or pyroelectric). The equation is given in a form suitable for modern methods of experimental data interpretation.

2. As was shown in [3], the energy flux per unit area of the sensing element of the thermal transducer is determined by the expression

$$W = J[\varkappa(E_c + E_B - E_S) + (1 - \varkappa)\xi(E_c - E_e)], \tag{2.1}$$

where $E_c = mv^2/2 + E_i$, where J is the molecular flux density, m, v and $E_i$ are the molecular mass, velocity, and intrinsic energy, respectively, $\varkappa$ is the capture coefficient, $E_B$ is the sublimation energy, $E_e$ is the energy of molecules in the state of thermal equilibrium with the surface, $\xi$ is the accommodation factor, and $E_S$ is the molecular energy in the solid condensate phase at the surface.

For most gases and the deep-frozen, superconducting bolometers used in [1-6], expression (2.1) is considerably simplified in view of the fact that $\varkappa = 1$ and $E_S \ll E_c$ with sufficiently high accuracy. In this case (2.1) can be approximated by the expression

$$W = J(E_c + E_B). \tag{2.2}$$

The case where $E_i \gtrsim E_B$ and, as a result of liberation of intrinsic energy, $\varkappa \neq 1$ and $\xi \neq 1$ is not considered here.

Novosibirsk. Translated from Zhurnal Prikladnoi Mekhaniki i Tekhnicheskoi Fiziki, No. 2, pp. 45-49, March-April, 1985. Original article submitted February 22, 1984.

0021-8944/85/2602-0191$09.50  